A Luminogen with Aggregation-Induced Emission Characteristics for Wash-Free Bacterial Imaging, High-Throughput Antibiotics Screening and Bacterial Susceptibility Evaluation

*Engui Zhao, Yilong Chen, Sijie Chen, Haiqin Deng, Chen Gui, Chris W. T. Leung, Yuning Hong, Jacky W. Y. Lam, and Ben Zhong Tang**

Bacteria exist everywhere and are intimately related to human life in all aspects, including food and water, medical treatment, healthcare, environment, and so on.[1] Most bacteria are benign to human beings and some of them are even beneficial to human health. For example, some *Escherichia coli* (*E. coli*) in our intestinum crassum can produce vitamin B and K, which are necessities for human to perform normal physiological functions. Some species of bacteria, however, are harmful or even fetal. There has been a battle between human and these harmful bacteria throughout the human history. Before the discovery of antibiotics, human beings were impotent in most of antagonisms with these harmful bacteria. Antibiotics came into power as the weapon of human immediately after their discoveries.[2,3] These weapons, however, are losing their forces gradually with the increasing emergence of antibiotic resistance.[4–6] In order to alleviate or resolve the antibiotic resistance issues, effort should be devoted to the development of fast methods for evaluation of bacterial susceptibility and new effective antibiotics for infection prevention and treatment.[7,8] The former will guide doctors to select the best candidate for infection treatment and even provide personalized treatment, while the later can eliminate bacteria that are resistant to traditional antibiotics, even superbugs. Both these two developments rely on bacterial experiments.

Traditional methods for bacterial susceptibility evaluation and antibiotics screening, such as disk diffusion, agar dilution, broth microdilution, etc.,[9] require tedious labor work in superpurgative working table and long incubation time of 24 to 48 h to allow bacterial growth for identification. To circumvent these limitations, some new methods are developed on the basis of other techniques, such as electrochemical measurement,[10] real-time PCR,[11–13] etc. However, ponderous machinery setup and tedious operation are needed, and the obtained results suffer from unsatisfied sensitivity and reproducibility. Thus, reliable methods for fast bacterial susceptibility evaluation and antibiotics screening are still in urgent need.

Fluorescence enjoys the advantages of high sensitivity and selectivity, non-invasion, and less interference, and is thus widely used in sensory, imaging, and screening applications. Taking advantage of the Förster resonance energy transfer (FRET) technique, Wang and co-workers developed a fluorescence-based method for high-throughput antibiotics screening and bacterial susceptibility evaluation.[14,15] However, in their method, washing process is needed to wash away the culture medium before quantification by fluorescence, which increases the experimental procedures and decreases the accuracy due to the loss of bacteria during washing process (Scheme S1, Supporting Information). Moreover, the non-linear relationship of the FRET ratio with respect to the bacteria concentration increases the difficulties in determining the parameters that denote antibiotics effectiveness, such as half maximal inhibitory concentration (IC_{50}) and minimum inhibitory concentration (MIC).

Recently, a unique phenomenon of aggregation-induced emission (AIE) was observed on a species of propeller-shaped molecules, which emit faintly in their solutions, but fluoresce intensely in the aggregated state.[16] Through systematic studies, restriction of intramolecular motion (RIM) was identified as the main cause for the AIE effect.[17,18] These AIE luminogens (AIEgens)[19] show great potential in biological research, and lots of biological applications have been developed with these materials, including cell[20–23] and bacteria[24,25] imaging, tissue[26] and tumor visualization,[27,28] therapy,[29–32] and drug

E. Zhao, Dr. Y. Chen, Dr. S. Chen, H. Deng, C. Gui, C. W. T. Leung, Dr. Y. Hong, Dr. J. W. Y. Lam, Prof. B. Z. Tang
HKUST Shenzhen Research Institute
Nanshan, Shenzhen 518057, China
E-mail: tangbenz@ust.hk

E. Zhao, Dr. Y. Chen, Dr. S. Chen, H. Deng, C. Gui, C. W. T. Leung, Dr. Y. Hong, Dr. J. W. Y. Lam, Prof. B. Z. Tang
Division of Biomedical Engineering
Department of Chemistry
Institute for Advanced Study
Division of Life Science
State Key Laboratory of Molecular Neuroscience
and Institute of Molecular Functional Materials
The Hong Kong University of Science & Technology (HKUST)
Clear Water Bay
Kowloon, Hong Kong, China

Prof. B. Z. Tang
Guangdong Innovative Research Team
SCUT-HKUST Joint Research Laboratory
State Key Laboratory of Luminescent Materials and Devices
South China University of Technology (SCUT)
Guangzhou 510640, China

DOI: 10.1002/adma.201501972

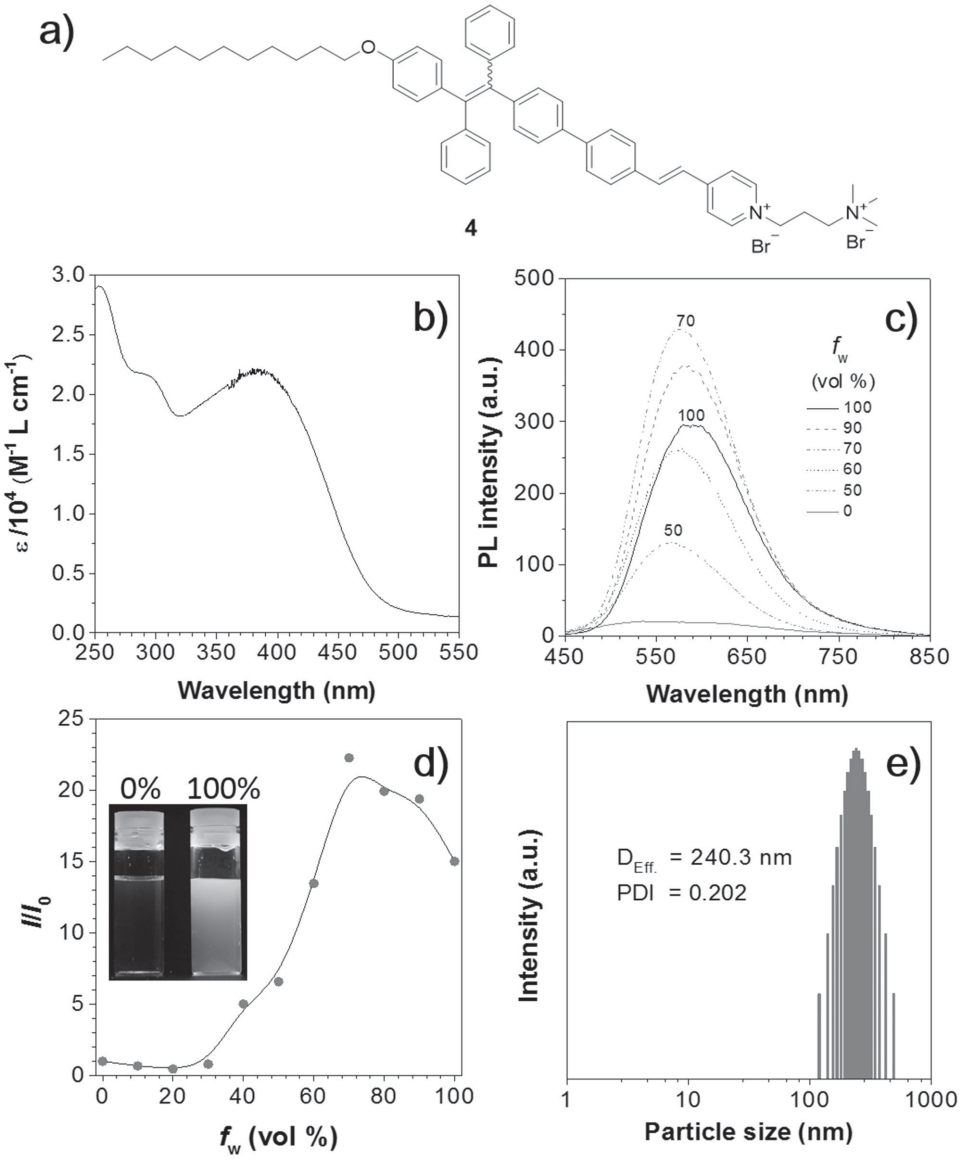

Figure 1. a) Molecular structure of **4**. b) UV–vis absorption spectrum of the aqueous solution of **4**. c) PL spectra of **4** in DMSO/water mixtures with different water fractions (f_w). Concentration: 50×10^{-6} M; excitation wavelength: 405 nm. d) Plot of PL intensity versus the composition of the DMSO/water mixtures of **4**. Inset: photographs of DMSO/water mixtures of **4** with different water fractions taken under 365 nm UV irradiation. e) Particle size of aggregates of **4** formed in an aqueous solution. Concentration: 40×10^{-6} M.

delivery.[33,34] The fluorescence turn-on characteristics of the AIEgens upon binding to the targets make them excellent candidates as fluorescence sensors and inspire us to explore their potentials in bacterial susceptibility evaluation and antibiotics screening. In this work, we report a facile and fast method for bacterial susceptibility evaluation and high-throughput antibiotics screening with the aid of a new AIEgen (**4**) (**Figure 1**a).

A new AIEgen **4** was synthesized following the procedures reported previously (Scheme S2, Supporting Information).[25] The cross McMurry coupling reaction of 4-hydroxybenzophenone and 4-bromobenzophenone gave **1**, which then underwent Williamson ether synthesis reaction by treatment of 1-bromoundecane to form **2**. Compound **2** was transformed to **3** by Suzuki coupling reaction with 4-bromobenzaldehyde. The subsequent condensation between **3** and pyridinium salt produced **4**. All the intermediates and **4** were obtained in medium to high yields and characterized by ^{1}H NMR, ^{13}C NMR, and HRMS, from which satisfactory results corresponding to their molecular structures were obtained (Figure S1, Supporting Information).

The aqueous solution of **4** displays an absorption band peaked at 386 nm (Figure 1b), which is red-shifted by ca. 60 nm compared with tetraphenylethene (TPE). The ether group is electron-donating, while the pyridium salt is strongly electron-withdrawing. The donor-acceptor interaction across the TPE core facilitates the electron mobility and lowers the energy gap,

resulting in the bathochromic shift in the absorption spectrum. **4** is a typical AIE-active molecule. Its DMSO solution is almost non-emissive (Figure 1c). Gradually increasing the water fraction (f_w) leads to aggregate formation and turns on the fluorescence of **4**. The photoluminescence (PL) intensity of its DMSO/H_2O mixture with f_w of 70% is more than 22 times higher than that of its DMSO solution (Figure 1d). The emission intensity drops at f_w of higher than 70%, presumably owing to precipitation, which leads to decreased effective concentration and recorded emission intensity.

The positively charged amines and the long alkyl chain endow **4** with the hydrophilicity and hydrophobicity, respectively, making it an amphiphilic molecule. It is dissolved in water at low concentrations, but forms micelles at high concentrations. Taking advantage of the AIE characteristics, the critical micelle concentration (CMC) can be determined facilely (Figure S2, Supporting Information).[25] Plotting the fluorescence intensity versus the concentration of **4** gives an estimation of CMC to be ca. 20×10^{-6} M. The nanoaggregates formed at a concentration higher than CMC were characterized by the ζ-potential analyzer (Figure 1e). Particles with effective diameter of 240.3 nm were detected with a polydispersity index of 0.202. The nanoaggregates were further examined by transmission electron microscopy (TEM) measurement. Black spots with sizes of 100–200 nm are clearly observed in the TEM image (Figure S3, Supporting Information), which corroborates the aggregate formation of **4**.

4 bears two amine groups and is positively charged, while the bacterial cell envelop is negatively charged. The electrostatic interaction between **4** and bacterial cell envelope is playing a key role in the bacterial imaging process. At concentrations below CMC, **4** molecularly presents in its aqueous solutions and thus fluoresces faintly, owing to its AIE characteristics. In the presence of bacteria, **4** binds to these bacteria driven by the electrostatic force and its fluorescence is turned on. As shown in **Figure 2**b, Gram-positive bacteria, *Staphylococcus epidermidis* (*S. epidermidis*), are imaged clearly under the fluorescence microscope after incubation with 10×10^{-6} M of **4** for 10 min. Thanks to its AIE characteristics, the unbound molecules of **4** remain non-fluorescent and only these bound to bacteria are lighted up. Thus, without washing process, the background emission is very low, which simplifies the imaging process, avoids bacteria loss during the washing process and thus increases the accuracy in bacterial quantification. Then, we applied **4** to the imaging of Gram-negative bacteria, *E. coli*. As shown in Figure 2d, under the same staining conditions, *E. coli* are visualized clearly under the fluorescence microscope. The results indicate that **4** stains both Gram-positive and Gram-negative bacteria.

We then applied **4** to the detection of bacteria in bulk solutions. In these experiments, a MOPS/ethanol (8:2 v/v) mixture was utilized, in which MOPS is a defined bacterial culture medium and ethanol can stabilize the fluorescence signal and decrease the background emission due to the better solubility of **4** in ethanol. As shown in Figure 2e, the solution containing *S. epidermidis* displays a bright orange emission, whilst that without bacteria is almost non-emissive. The difference can be clearly distinguished by naked eyes. To quantify the difference in fluorescence intensity, we measured the PL spectra of these bulk solutions (Figure 2f). The solution of **4** and *S. epidermidis*

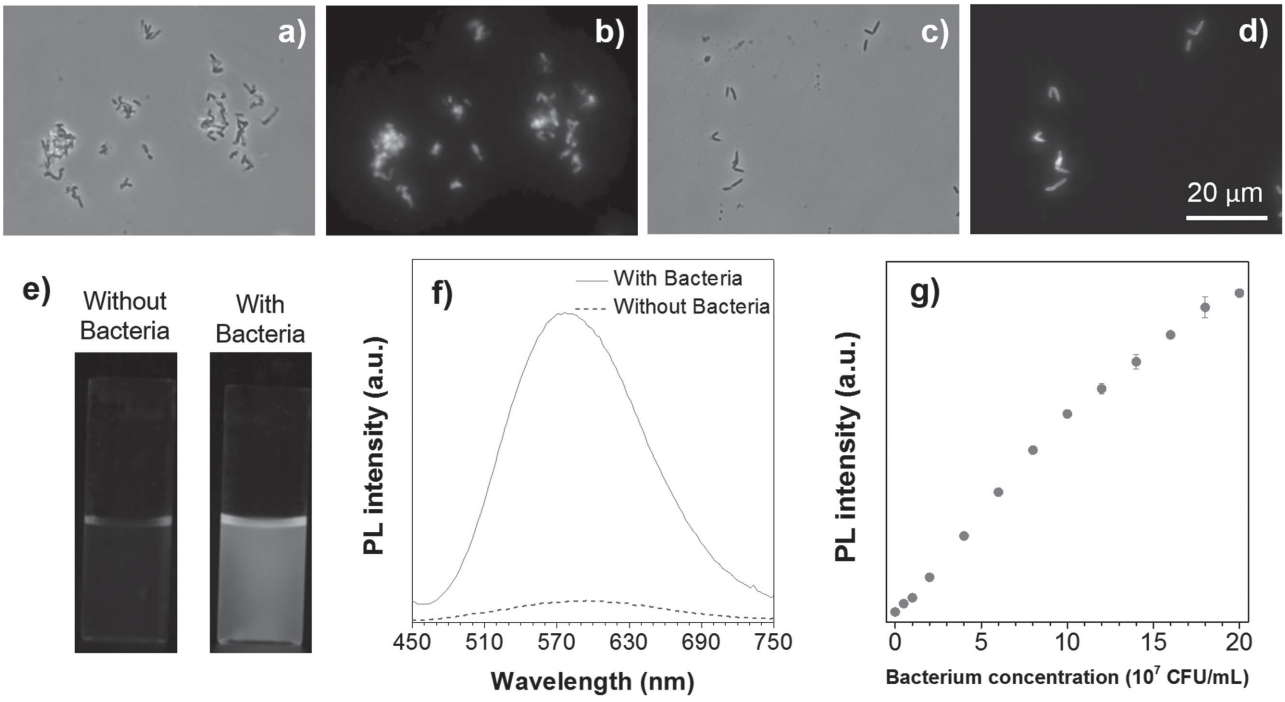

Figure 2. a,c) Bright–field and b,d) fluorescence images of (a,b) *S. epidermidis* and (c,d) *E. coli* incubated with 10×10^{-6} M of **4** for 10 min. Excitation wavelength: 400–440 nm. e) Photographs of MOPS/ethanol (8:2, v/v) solution of **4** with/without 10^8 CFU mL^{-1} of *S. epidermidis* taken under 365 nm UV irradiation. f) PL spectra of MOPS/ethanol (8:2, v/v) mixture of **4** with/without 10^8 CFU mL^{-1} of *S. epidermidis*. Excitation wavelength: 430 nm. g) Change in PL intensity of **4** with the concentration of *S. epidermidis* in MOPS/ethanol (8:2, v/v) mixture. Excitation wavelength: 430 nm.

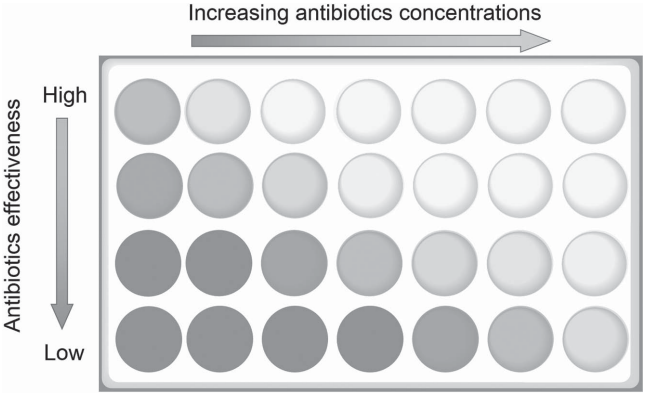

Scheme 1. Illustration of high-throughput antibiotics screening strategy.

displays 15 times higher emission intensity than that of **4** alone. We then investigated the fluorescence response of **4** to different concentrations of *S. epidermidis*. Interestingly, the PL intensity of **4** takes linear relationship with bacteria concentrations in the range of 5×10^6 to 2×10^8 CFU mL^{-1} (Figure 2g). The detection limit is estimated to be ca. 5.5×10^5 CFU mL^{-1} from the low concentration region (0–10^8 CFU mL^{-1}) of Figure 2g. The fluorescence turn-on visualization of bacteria, simple imaging procedures with enhanced accuracy and large linear relationship region enable its high-throughput antibiotics screening applications.

The design principle of employing **4** for antibiotics screening is shown in **Scheme 1**. Without antibiotics, bacteria grow rapidly under suitable conditions. Effective antibiotics will retard or completely inhibit the growth of bacteria. Thus, after designed incubation time the total bacteria amount will remain unchanged. Addition of **4** in culture medium will result in low emission intensity of **4**, since most of them molecularly present in the culture medium and emit weakly. Ineffective antibiotics, however, will not affect bacterial growth significantly. Addition of **4** at the end of bacterial culture will lead to strong fluorescence due to the presence of large amount of bacteria. Since the PL intensity of **4** is in linear relationship with bacteria concentration, bacteria amount in these culture media containing different antibiotics can be easily identified by measuring the fluorescence intensity of these culture solutions, from which some important parameters describing the antibiotic effectiveness, such as IC_{50} and MIC can be determined facilely.

To test the feasibility of the strategy mentioned above, six antibiotics were utilized, which were ampicillin sodium salt (AMP), kanamycin sulfate (KANA), streptomycin sulfate (STM), colistin (CLS), gentamicin sulfate (GEN), spectinomycin dihydrochloride pentahydrate (SPM). We first cultured bacteria in MOPS for different periods of time to identify suitable culturing time. Gram-positive bacteria, *S. epidermidis* were cultured for different periods of time, followed by addition of **4** and determination of the fluorescence enhancement $((I - I_0)/I_0)$. As shown in Figure S4, Supporting Information, with the increase in incubation time, the fluorescence enhancement became larger. In our experiments, we chose 4 h for conducting the following experiments to make sure that the fluorescence difference is large enough for giving reliable results. However, the incubation time can be shortened to a large extent

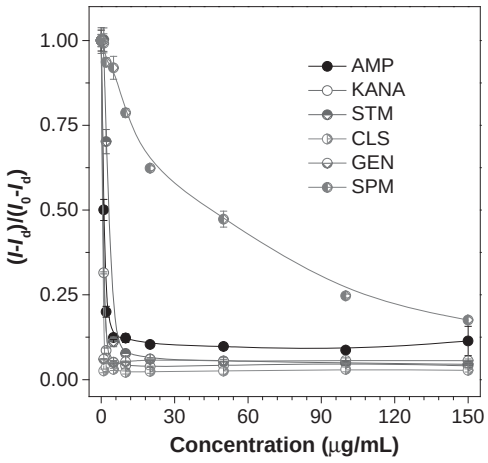

Figure 3. Evaluation of the effectiveness of different antibiotics on *S. epidermidis*. *S. epidermidis* was first incubated with different concentrations of antibiotics, followed by quantification with **4** in MOPS/ethanol (8:2, v/v) mixture. Excitation wavelength: 430 nm.

at the expense of the fluorescence enhancement. Then, we examined the interference of these antibiotics to the PL intensities of **4**. As shown in Figure S5, Supporting Information, antibiotics alone with concentrations of up to 150 μg mL^{-1} do not lead to an obvious increase in emission intensity. Afterward, *S. epidermidis* were grown in MOPS in the presence of antibiotics at varied concentrations. After 4 h, **4** dissolved in ethanol was added into the culture solutions to reach a final concentration of 10×10^{-6} M and ethanol volume fraction of 20%. The mixtures were then subjected to fluorescence measurement to obtain the relative fluorescence intensities $((I - I_d)/(I_0 - I_d))$ of experimental groups $(I - I_d)$ with respect to the control group $(I_0 - I_d)$ in which no antibiotic was added (**Figure 3**). I_d is the fluorescence intensity of MOPS/ethanol mixture with **4** alone. Since the fluorescence intensity is in linear relationship with bacteria concentration, the plots represent the changes of bacteria amount with antibiotics concentrations. From the plots, MIC and IC_{50} are determined easily and the obtained values for the tested antibiotics are summarized in **Table 1**. AMP, STM, CLS, and GEN are all very effective antibiotics with IC_{50} and MIC values of less than or equal to 1 and 5 μg mL^{-1}, respectively. STM exhibits higher IC_{50} and MIC values of 3 and 10 μg mL^{-1}, respectively. SPM displays IC_{50} and MIC values of larger than 20 and 150 μg mL^{-1}, respectively. These results demonstrate that AMP, KANA, STM, CLS, and GEN are effective antibiotics against *S. epidermidis*, while SPM is not. To verify these results, the broth microdilution method was applied to determine the IC_{50} and MIC values of KANA and SPM, from

Table 1. Results of susceptibility of *S. epidermidis* toward different antibiotics.

Antibiotics	AMP	KANA	STM	CLS	GEN	SPM
IC_{50} [μg mL^{-1}]	1	<1	3	<1	<1	>20
MIC [μg mL^{-1}]	5	<5	10	<1	<1	>150
Susceptibility[a)]	S	S	S	S	S	R

[a)]S: susceptible; R: resistant.

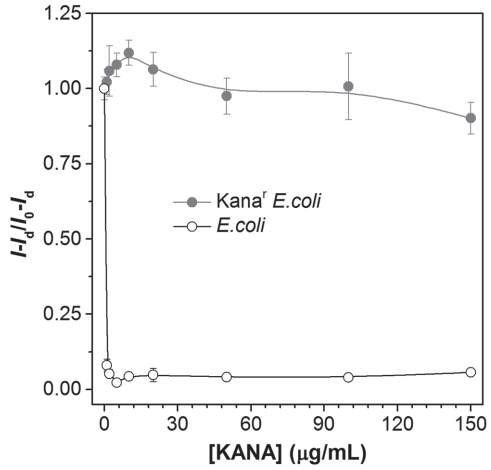

Figure 4. Evaluation of the susceptibility of *E. coli* and Kana^r *E. coli* toward KANA. Excitation wavelength: 430 nm.

which similar IC_{50} and MIC values were obtained. The results corroborate the reliability of the fluorescence method for antibiotics screening employing **4** as the probe. In our method, less than 5 h is needed to obtain these parameters, while it takes more than 24 h for the broth dilution method to give similar results.

Taking this strategy, bacterial susceptibility can be evaluated. To illustrate this process, two bacteria strains, *E. coli* and Kana^r *E. coli* (KANA-resistant *E. coli*) were applied. For *E. coli*, low concentration of KANA inhibited its growth, thus low fluorescence was obtained (**Figure 4**). For Kana^r *E. coli*, high concentrations of KANA remained ineffective, thus leading to strong fluorescence at KANA concentration of up to 150 μg mL^{-1}. In this way, Kana^r *E. coli* can be clearly distinguished from *E. coli* and the susceptibility of bacteria can be evaluated facilely.

To sum up, we developed a new AIEgen (**4**), which can image both Gram-positive and negative bacteria without the involvement of washing process. In this way, bacteria loss during the washing process is avoided and the accuracy for bacterial identification is increased. **4** can also be applied to high-throughput antibiotics screening and bacterial susceptibility evaluation. Reliable results can be obtained within 5 h, which is greatly shortened compared with traditional methods. The new method may contribute to the development of new antibiotics and lay the foundation for personalized diagnosis and prescription.

Experimental Section

Materials: LB agar, LB broth, potassium phosphate dibasic anhydrous, and sodium phosphate were purchased from USB Co. Zinc dust, titanium tetrachloride, 4-hydroxybenzophenone, 4-bromobenzophenone, 1-bromoundecane, potassium carbonate, 4-formylphenylboronic acid, tetrakis(triphenylphosphine)palladium, and piperidine were purchased from Sigma–Aldrich and used as received. THF was purified by distillation from sodium benzophenone ketyl immediately prior to use. 1-(3-Trimethylammoniopropyl)-4-methylpyridinium dibromide was synthesized according to the literature method.[35] Other reagents used in this work, such as amino acids, nucleotides, vitamins, potassium chloride, and sodium chloride were purchased from Sigma–Aldrich or other companies.

Characterization: ^1H and ^{13}C NMR spectra were measured on Bruker ARX 400 NMR spectrometers using $CDCl_3$ or DMSO-d_6 as the deuterated solvents. High-resolution mass spectra (HRMS) were recorded on a Finnigan MAT TSQ 7000 Mass Spectrometer System operating in a MALDI-TOF mode. UV–vis absorption spectrum was taken on a Milton Ray Spectronic 3000 array spectrophotometer. Steady-state fluorescence spectra were recorded on a Perkin–Elmer LS 55 spectrofluorometer. Fluorescence images were collected on Olympus BX 41 fluorescence microscope. Particle sizes were measured on a Zeta potential analyzer (Brookhaven, ZETAPLUS). The aggregate morphology of TPE-Bac was investigated using transmission electron microscopy (Japan, JEOL JEM 100CXII) at an accelerating voltage of 100 kV. The high-throughput fluorescence assays were performed in a 96-well microtiter plate measured by a Perkin–Elmer Wallac Victor 1420 Multilabel Counter using 430 and 535 nm as excitation and emission wavelengths, respectively.

Synthesis: 1-(4-Bromophenyl)-2-(4-Hydroxyphenyl)-1,2-Diphenylethene (1): **1** was synthesized following the procedures reported in the literature,[36] with some modifications. 4-Hydroxybenzophenone (1.98 g, 10 mmol), 4-bromobenzophenone (5.20 g, 20 mmol), and zinc dust (5.88 g, 90 mmol) were added into a 500 mL two-necked round-bottum flask equipped with a condenser, which was evacuated under vacuum and flushed with dry nitrogen for three times. After addition of 200 mL of THF, the mixture was cooled to −78 °C in acetone/dry ice bath. $TiCl_4$ was then added dropwise at −78 °C. Afterward, the mixture was refluxed overnight under nitrogen. After cooling to room temperature, the mixture was acidified with aqueous HCl solution (1 M) to pH < 2. The organic mixture was extracted with dichloromethane (DCM) and dried with anhydrous sodium sulfate. After filtration and solvent evaporation, the crude product was purified by silica gel column chromatography using hexane/ethyl acetate (10:1 v/v) as eluting solvent to give **1** as a white solid (3.1 g, 72%). ^1H NMR (400 MHz, $CDCl_3$, δ): 7.25–7.19 (m, 2H), 7.14–6.98 (m, 10H), 6.92–6.86 (m, 4H), 6.60–6.55 (m, 2H), 4.885 (d, 1H, OH). ^{13}C NMR (100 MHz, $CDCl_3$, δ): 153.66, 153.55, 142.93, 142.88, 142.85, 142.35, 142.26, 140.47, 138.24, 138.20, 135.38, 135.27, 132.36, 132.06, 132.04, 130.64, 130.27, 130.17, 127.22, 127.11, 127.02, 126.04, 125.94, 125.87, 119.63, 114.18, 113.99. HRMS (MALDI-TOF) *m/z*: calcd for $C_{26}H_{19}BrO$, 426.0619 [M]; found, 428.0613 $[M+2H]^+$.

1-(4-Bromophenyl)-2-(4-Undecyloxyphenyl)-1,2-Diphenylethene (2): Into a 250 mL two-necked round bottom flask were added potassium carbonate (4.00 g, 28.25 mmol) and **3** (2.5 g, 5.65 mmol). The flask was vacuumed and purged with dry nitrogen for three times. After adding 1-bromoundecane (2.66 g, 11.3 mmol) and DMF (80 mL), the reaction mixture was stirred overnight at 70 °C under nitrogen condition. After cooling down to room temperature, the mixture was extracted with DCM, washed with distilled water several times and dried with anhydrous magnesium sulfate. The crude product was purified by running silica gel column chromatography using hexane and DCM (v/v, 10/1) as eluting solvent to give **2** as light yellow viscous oil (2.62 g, 80%). ^1H NMR (400 MHz, $CDCl_3$, δ): 7.27–7.18 (m, 2H), 7.15–7.07 (m, 6H), 7.05–6.97 (m, 4H), 6.94–6.85 (m, 4H), 6.68–6.60 (m, 2H), 3.92–3.84 (m, 2H), 1.80–1.63 (m, 2H), 1.48–1.22 (m, 16H), 0.92–0.86 (t, 3H); ^{13}C NMR (100 MHz, $CDCl_3$, δ): 157.285, 157.197, 143.074, 143.004, 142.963, 142.877, 142.443, 142.389, 140.659, 140.639, 138.029, 137.984, 134.896, 134.792, 132.382, 131.827, 131.802, 130.701, 130.672, 130.256, 130.146, 127.202, 127.171, 127.084, 126.974, 125.977, 125.874, 125.800, 119.557, 113.129, 112.958, 67.237, 67.188, 63.501, 31.278, 28.979, 28.862, 28.803, 28.784, 28.709, 28.557, 27.881, 25.435, 25.424, 25.189, 22.058, 13.493; HRMS (MALDI-TOF) *m/z*: calcd for $C_{37}H_{41}BrO$, 580.2341 [M]; found, 580.2346 $[M]^+$.

4′-(1,2-Diphenyl-2-(4-(Undecyloxy)Phenyl)Vinyl)-[1,1′-Biphenyl]-4-Carbaldehyde (3): Into a 250 mL two-necked round bottom flask were added **2** (2.60 g, 3.50 mmol), 4-formylphenylboronic acid (0.82 g, 5.47 mmol), K_2CO_3 (3.14 g, 22.72 mmol) and $Pd(PPh_3)_4$ (0.31 g, 0.27 mmol). The flask was vacuumed and purged with nitrogen for three times. Afterward, THF (80 mL) and water (20 mL) were injected into the flask, followed by refluxing overnight under nitrogen condition. After

cooling down to room temperature, the mixture was extracted with DCM, washed with distilled water several times and dried with anhydrous magnesium sulfate. The crude product was purified by running silica gel column chromatography using hexane and DCM (v/v, 5/1) as eluting solvent to give **3** as yellow viscous oil (1.76 g, 83%).^{1}H NMR (400 MHz, $CDCl_3$, δ): 10.04 (s, –CHO), 10.03 (s, –CHO), 7.95–7.89 (t, 2H), 7.75–7.68 (m, 2H), 7.47–7.39 (m, 2H), 7.23–7.09 (m, 12H), 7.05–6.97 (m, 2H), 6.73–6.66 (m, 2H), 3.93–3.88 (t, 2H), 1.82–1.73 (m, 2H), 1.52–1.27 (m, 16H), 0.97–0.91 (m, 3H); ^{13}C NMR (100 MHz, $CDCl_3$, δ): 191.176, 157.373, 157.278, 146.050, 144.064, 143.993, 143.321, 143.292, 143.233, 140.828, 138.610, 138.572, 136.425, 135.105, 134.446, 131.997, 131.503, 130.873, 130.838, 129.628, 129.609, 127.301, 127.220, 127.178, 127.064, 126.718, 126.010, 125.948, 125.900, 125.861, 113.183, 113.046, 67.240, 31.351, 29.061, 29.019, 28.873, 28.785, 28.745, 25.510, 22.140, 13.609; HRMS (MALDI-TOF) *m/z*: calcd for $C_{44}H_{46}O_2$, 606.3498 [M]; found, 606.3506 [M]$^+$.

*4-((1E)-2-(4′-(1,2-Diphenyl-2-(4-(Undecyloxy) Phenyl)vinyl)-[1,1′-Biphenyl]-4-yl) Vinyl)-1-(3-(Trimethylammonio) Propyl) Pyridin-1-ium Bromide (**4**)*: A solution of 1-(3-trimethylammoniopropyl)-4-methylpyridinium dibromide (0.30 g, 0.85 mmol) and **3** (1 g, 1.63 mmol) was refluxed under nitrogen in dry ethanol catalyzed by three drops of piperidine. After cooling to room temperature, the solvent was removed by evaporation under reduced pressure. The residue was purified by a silica gel column chromatography using DCM and methanol mixture (2:1 v/v) as eluting solvent to give a red powder of **4** (0.38 g, 47%). ^{1}H NMR (400 MHz, DMSO-d_6, δ): 8.92 (d, 2H), 8.26 (d, 2H), 8.05 (d, 1H), 7.82–7.71 (m, 4H), 7.59–7.49 (m, 3H), 7.17–6.79 (m, 15H), 6.69–6.61 (dd, 2H), 4.59–4.51 (m, 2H), 3.84–3.78 (m, 2H), 3.42–3.35 (m, 3H), 3.06 (s, 9H), 2.46–2.36 (m, 2H), 1.64–1.54 (m, 2H), 1.36–1.14 (m, 16H), 0.83–0.76 (m, 3H); ^{13}C NMR (100 MHz, DMSO-d_6, δ): 157.045, 153.071, 144.138, 143.292, 143.229, 143.160, 140.954, 140.504, 140.465, 138.858, 136.337, 134,971, 133.914, 131.733, 131.273, 130.540, 128.727, 127.792, 127.723, 127.583, 126.714, 126.515, 126.354, 125.784, 125.698, 123.738, 122.915, 113.633, 113.474, 67.055, 61.605, 56.400, 55.883, 52.338, 31.063, 28.727, 28.470, 28.413, 25.259, 23.949, 21.877, 21.866, 18.254, 13.749; HRMS (MALDI-TOF) *m/z*: calcd for $C_{56}H_{66}Br_2N_2O$, 861.4353 [M-Br]$^+$; found, 861.4343 [M-Br]$^+$.

Sample Preparation: A stock solution of **4** in DMSO with a concentration of 10×10^{-3} M was prepared and stocked in the 4 °C fridge. The stock solution was diluted to 50×10^{-6} M with ethanol prior to use. MOPS E/Z rich defined medium was prepared according to the protocol given on the *E. coli* genome project. Phosphate buffer saline (PBS) was prepared by dissolving NaCl (8 g), KCl (0.2 g), Na_2HPO_4 (1.44 g), and KH_2PO_4 (0.24 g) in 800 mL distilled water, adjusting pH to 7.4 with HCl, and calibrating to 1 L by adding H_2O. PBS was sterilized by autoclaving for 20 min at 15 psi (1.05 kg cm^{-2}) on liquid cycle and stored at room temperature.

Bacterial Culturing and Staining: A single colony of bacteria on solid culture medium [Luria broth (LB) for *E. coli* and *S. epidermidis*] was transferred to 5 mL of liquid culture medium and grown at 37 °C for 10 h. The concentrations of bacteria were determined by measuring optical density at 600 nm (OD_{600}) and then 10^9 colony forming unit (CFU) (1 $OD_{600} = 10^9$ CFU mL^{-1}) of bacteria were transferred to a 1.5 mL EP tube. Bacteria were harvested by centrifuging at 5000 rpm for 3 min. After removal of supernatant, 1 mL of **4** in PBS solution at the concentration of 10×10^{-6} M was added into the EP tube. After dispersing with vortex, the bacteria were incubated at room temperature for 10 min.

Bacterial Imaging: To take fluorescence images, about 4 µL of stained bacteria solution was transferred to glass slide and then covered by a coverslip. The image was collected using 100× objective. The bacteria were imaged under a FL microscope (BX41 Microscope) using 400–440 nm excitation filter, 455 nm dichroic mirror, and 465 nm long pass emission filter.

Standard Curve: Into 1 mL MOPS culture medium was added different concentrations of bacteria (from 5×10^6 up to 2×10^8 CFU mL^{-1}), then 0.25 mL ethanol solution of **4** (50×10^{-6} M) was added to the bacteria solutions. The solutions were then subjected to incubation in 37 °C incubator for 10 min. Then the solutions were allocated into 96-well microtiter plate, followed by measuring by multilabel counter using 430 and 535 nm as excitation and emission wavelengthes, respectively. The fluorescence of **4** in MOPS/ethanol (8:2, v/v) mixture without bacteria was also measured for control. The detection limit was calculated by 3 × standard deviation of low concentration/slope of the calibration line.

High-Throughput Antibiotics Screening: Fresh MOPS culturing medium was added into EP tube. Then, antibiotics to be screened and 5×10^6 CFU bacteria were introduced to the MOPS culturing medium. The final volume of each tube was 1 mL. The innoculated bacteria solution was kept at 37 °C for 4 h. Afterward, 0.25 mL ethanol solution of **4** (50×10^{-6} M) was added to the bacteria solutions, which was then subjected to incubation at 37 °C for 10 min. Then the solutions were allocated into 96-well microtiter plate, followed by measuring of fluorescence intensity employing multilabel counter using 430 and 535 nm as excitation and emission wavelengths, respectively.

Supporting Information

Supporting Information is available from the Wiley Online Library or from the author.

Acknowledgements

E.Z. and Y.C. contributed equally to this work. This work was in part supported by the National Basic Research Program of China (973 Program, 2013CB834701), the University Grants Committee of Hong Kong (AoE/P-03/08), the Research Grants Council of Hong Kong (604913, 16301614 and N_HKUST604/14), the Innovation and Technology Commission (ITCPD/17–9), the Science and Technology Plan of Shenzhen (JCY)20140425170011516), and the Natural Science Fund of Guangdong Province (2014A030313659). The authors thank the support of the Guangdong Innovative Research Team Program (201101C0105067115).

Note: The labeling of the curves in Figure 4 was incorrect when the article was initially published: this was corrected on September 2, 2015.

Received: April 24, 2015
Revised: June 18, 2015
Published online: July 14, 2015

[1] D. Ivnitski, I. Abdel-Hamid, P. Atanasov, E. Wilkins, *Biosens. Bioelectron.* **1999**, *14*, 599.
[2] L. L. Ling, T. Schneider, A. J. Peoples, A. L. Spoering, I. Engels, B. P. Conlon, A. Mueller, D. E. Hughes, S. Epstein, M. Jones, L. Lazarides, V. A. Steadman, D. R. Cohen, C. R. Felix, K. A. Fetterman, W. P. Millett, A. G. Nitti, A. M. Zullo, C. Chen, K. Lewis, *Nature* **2015**, *517*, 455.
[3] J. L. Martínez, F. Baquero, D. I. Andersson, *Nat. Rev. Microbiol.* **2007**, *5*, 958.
[4] G. Cox, G. D. Wright, *Int. J. Med. Microbiol.* **2013**, *303*, 287.
[5] F. E. Koehn, G. T. Carter, *Nat. Rev. Drug Discovery* **2005**, *4*, 206.
[6] J. D. D. Pitout, K. B. Laupland, *Lancet Infect. Dis.* **2008**, *8*, 159.
[7] G. D. Wright, D. T. Hung, J. D. Helmann, *Nat. Med.* **2013**, *19*, 544.
[8] M. R. Hamblin, T. Hasan, *Photochem. Photobiol. Sci.* **2004**, *3*, 436.
[9] A. C. Gales, A. O. Reis, R. N. Jones, *J. Clin. Microbiol.* **2001**, *39*, 183.
[10] P. Ertl, E. Robello, F. Battaglini, S. R. Mikkelsen, *Anal. Chem.* **2000**, *72*, 4957.
[11] R. A. Forsyth, R. J. Haselbeck, K. L. Ohlsen, R. T. Yamamoto, H. Xu, J. D. Trawick, D. Wall, L. Wang, V. Brown-Driver, J. M. Froelich, G. C. Kedar, P. King, M. McCarthy, C. Malone, B. Misiner, D. Robbins, Z. Tan, Z.-Y. Zhu, G. Carr, D. A. Mosca, C. Zamudio, J. G. Foulkes, J. W. Zyskind, *Mol. Microbiol.* **2002**, *43*, 1387.

[12] M. A. Nadkarni, F. E. Martin, N. A. Jacques, N. Hunter, *Microbiology* **2002**, *148*, 257.
[13] F. J. Pérez-Pérez, N. D. Hanson, *J. Clin. Microbiol.* **2002**, *40*, 2153.
[14] C. Zhu, Q. Yang, L. Liu, S. Wang, *Angew. Chem. Int. Ed.* **2011**, *50*, 9607.
[15] H. Chen, B. Wang, J. Zhang, C. Nie, F. Lv, L. Liu, S. Wang, *Chem. Commun.* **2015**, *51*, 4036.
[16] J. Luo, Z. Xie, J. W. Y. Lam, L. Cheng, B. Z. Tang, H. Chen, C. Qiu, H. S. Kwok, X. Zhan, Y. Liu, D. Zhu, *Chem. Commun.* **2001**, *381*, 1740.
[17] Y. Hong, J. W. Y. Lam, B. Z. Tang, *Chem. Commun.* **2009**, 4332.
[18] Y. Hong, J. W. Y. Lam, B. Z. Tang, *Chem. Soc. Rev.* **2011**, *40*, 5361.
[19] J. Mei, Y. Hong, J. W. Y. Lam, A. Qin, Y. Tang, B. Z. Tang, *Adv. Mater.* **2014**, 1.
[20] C. W. T. Leung, Y. Hong, S. Chen, E. Zhao, J. W. Y. Lam, B. Z. Tang, *J. Am. Chem. Soc.* **2013**, *135*, 62.
[21] D. Ding, J. Liang, H. Shi, R. T. K. Kwok, M. Gao, G. Feng, Y. Yuan, B. Z. Tang, B. Liu, *J. Mater. Chem. B* **2014**, *2*, 231.
[22] X. Zhang, X. Zhang, B. Yang, M. Liu, W. Liu, Y. Chen, Y. Wei, *Polym. Chem.* **2014**, *5*, 356.
[23] H. Shi, R. T. K. Kwok, J. Liu, B. Xing, B. Z. Tang, B. Liu, *J. Am. Chem. Soc.* **2012**, *134*, 17972.
[24] E. Zhao, Y. Hong, S. Chen, C. W. T. Leung, C. Y. K. Chan, R. T. K. Kwok, J. W. Y. Lam, B. Z. Tang, *Adv. Healthcare Mater.* **2014**, *3*, 88.
[25] E. Zhao, Y. Chen, H. Wang, S. Chen, J. W. Y. Lam, C. W. T. Leung, Y. Hong, B. Z. Tang, *ACS Appl. Mater. Interfaces* **2015**, *7*, 7180.
[26] D. Wang, J. Qian, W. Qin, A. Qin, B. Z. Tang, S. He, *Sci. Rep.* **2014**, *4*, 4279.
[27] J. Zhang, C. Li, X. Zhang, S. Huo, S. Jin, F.-F. An, X. Wang, X. Xue, C. I. Okeke, G. Duan, F. Guo, X. Zhang, J. Hao, P. C. Wang, J. Zhang, X.-J. Liang, *Biomaterials* **2015**, *42*, 103.
[28] W. Qin, D. Ding, J. Liu, W. Z. Yuan, Y. Hu, B. Liu, B. Z. Tang, *Adv. Funct. Mater.* **2012**, *22*, 771.
[29] F. Hu, Y. Huang, G. Zhang, R. Zhao, H. Yang, D. Zhang, *Anal. Chem.* **2014**, *86*, 7987.
[30] C.-C. Chang, M.-C. Hsieh, J.-C. Lin, T.-C. Chang, *Biomaterials* **2012**, *33*, 897.
[31] Y. Yuan, G. Feng, W. Qin, B. Z. Tang, B. Liu, *Chem. Commun.* **2014**, *50*, 8757.
[32] E. Zhao, H. Deng, S. Chen, Y. Hong, C. W. T. Leung, J. W. Y. Lam, B. Z. Tang, *Chem. Commun.* **2014**, 1.
[33] X. Xue, Y. Zhao, L. Dai, X. Zhang, X. Hao, C. Zhang, S. Huo, J. Liu, C. Liu, A. Kumar, W.-Q. Chen, G. Zou, X.-J. Liang, *Adv. Mater.* **2014**, *26*, 712.
[34] C. Zhang, S. Jin, S. Li, X. Xue, J. Liu, Y. Huang, Y. Jiang, W.-Q. Chen, G. Zou, X.-J. Liang, *ACS Appl. Mater. Interfaces* **2014**, *6*, 5212.
[35] P. Yan, A. Xie, M. Wei, L. M. Loew, *J. Org. Chem.* **2008**, *73*, 6587.
[36] X.-F. Duan, J. Zeng, J.-W. Lue, Z.-B. Zhang, *Synthesis* **2007**, *5*, 713.